JOURNAL OF Applied Polymer SCIENCE

Relaxation behavior and activation energy of relaxation for polyimide and polyimide-graphene nanocomposite

Wajeeh F. Marashdeh, Jimmy Longun, Jude O. Iroh
Department of Mechanical and Materials Engineering, University of Cincinnati, Cincinnati, Ohio 45221-0021
Correspondence to: J. O. Iroh (E-mail: irohj@ucmail.uc.edu)

ABSTRACT: The relaxation behavior of polyimide and its nanocomposite containing 10 wt % of graphene was studied by using the dynamic mechanical spectrometer. Dynamic mechanical analysis of polyimide and its composite was performed as a function of temperature and frequency in the temperature range of 25–480 °C and frequency range between 0.05 and 100 Hz. The effect of increasing frequency of testing from 0.05 to 100 Hz is a significant shift from the glass transition temperature, T_g, to higher temperature from 360 °C at 0.05 Hz to 420 °C at 100 Hz. The tan δ peak height for both α and β transitions decreased with increasing test frequency from 0.24 at 0.05 Hz to 0.08 at 100 Hz, due to increasing restriction to chain motion. At any given testing frequency, the T_g for the composite was shown to be higher than that for the matrix by about 5–10 °C. The Arrhenius equation was used to calculate the activation energy for both α and β transitions. The activation for α and β transitions for the composite and polyimide matrix were determined to be 688 and 537 kJ/mol and 313 and 309 kJ/mol, respectively, indicating that a significant increase in the energy barrier to chain relaxation occurred as a result of reinforcement of polyimide with low weight fraction of graphene. © 2016 Wiley Periodicals, Inc. J. Appl. Polym. Sci. **2016**, *133*, 43684.

KEYWORDS: characterization; composites; glass transition; morphology; polyimides; properties

Received 4 December 2015; accepted 20 March 2016
DOI: 10.1002/app.43684

INTRODUCTION

Composite materials are increasingly used in the aerospace, aircraft, sports, and military industries because of their low density and outstanding specific modulus and strength. Because of their low density, there is a significant weight savings when composites are used in aircraft and automobile structures. Polymer matrix composites possess outstanding corrosion and fatigue damage resistance, thereby increasing device lifetime and durability.

Polyimides are classified as high-performance polymers,[1] because of their excellent mechanical properties, high temperature stability, and dimensional stability.[2,3] They are also reported to possess high strength, high modulus, and remarkable dielectric properties.[2–5] Consequently, polyimides and their composites are used in the construction of structural components in the automotive, transportation, and aerospace industries. Polyimides have also found a variety of applications in the military aircraft industry.[6] Polyimide (PI) is prepared from the reaction of a dianhydride with a diamine. Its chain backbone contains a characteristic cyclic imide functional group.[7] The formation of PI occurs in two steps, namely, (1) polymerization reaction to form the precursor, poly(amic acid) (PAA), and (ii) imidization or dehydrocyclization reaction which converts PAA into PI. Imidization is a cyclo-dehydration process that can occur thermally by heat treatment of poly(amic acid) or chemically by reaction with an anhydride.[8]

Recently, the discovery of graphene has provoked intensive attention due to the unique properties that can be derived from their nanoscale size and their high aspect ratio. Graphene, a single-layer carbon sheet with a hexagonal lattice structure, can be used as a filler to enhance the mechanical and physical properties of polyimide.[9–11] Dynamic mechanical analysis allows a rapid and accurate measurement of thermomechanical properties of thin films and moderately thick samples at a high strain rate (10^6 s^{-1}). The data obtained from dynamic mechanical analysis can be used to (1) predict the damping behavior of the material, (2) determine the extent of crosslinking, and (3) gain an insight into the chemical structure as well as the microstructure of a material. The dynamic mechanical analysis of polyimide and polyimide composites shows more than one structural relaxation over a wide range of temperatures.[12] However, the major secondary transition in polyimide is the α transition, which is observed at the glass transition region. The temperature corresponding to the α transition is taken to be the glass transition temperature T_g for a linear amorphous polymer. The glass transition region is the second region of viscoelastic

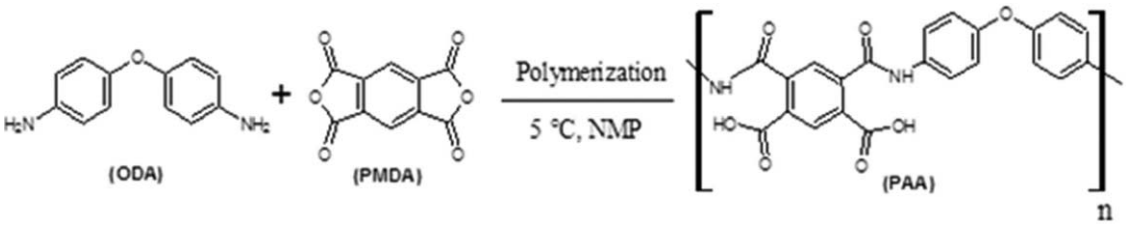

Figure 1. Synthesis of poly(amic acid).

behavior and it marks a change from glassy to rubbery behavior. In addition to the α transition, the other secondary transitions that could be observed at temperatures below the glass transition temperature, includes the β and γ transitions. The secondary relaxation phenomenon is usually studied by dynamic mechanical analysis and dielectric techniques.[13,14] Secondary transitions in polymers and polymer composites can be studied by calorimetric, free volume, static mechanical and dynamic mechanical methods. In this paper our focus is to use dynamic mechanical method to study the secondary transitions in polyimide and polyimide graphene composites. This approach seems more sensitive and reliable than the calorimetric method especially at high temperature $\geq$ 400 °C where the α transition in polyimide occurs. The difficulty in studying secondary transitions in high temperature polyimide using calorimetric method was also confirmed by others.[15] The activation enthalpy and the activation volume which reflect the sensitivity of plastic deformation has been calculated by using a variable strain rate method.[16]

In this study, the relaxation behavior of polyimide and polyimide-graphene composite containing 10 wt % of multilayered graphene is investigated as a function of test frequency and temperature. Polyimide nanocomposite containing 10 wt % of graphene was selected for this study because of its interesting optical, electrical, and mechanical properties. The activation energy for secondary transitions in polyimide and its nanocomposite was determined by using data obtained from dynamic mechanical analysis. Comparison of the damping behavior of polyimide and its nanocomposite was done by, comparing the shape of the Cole–Cole curve.

EXPERIMENTAL

Chemicals and Materials

The reagents used in this study include 4,4-oxydianiline (ODA, 97% purity), pyromellitic dianhydride (PMDA, 99% purity), and N-methyl-pyrrolidone (99% purity). They were purchased from Sigma–Aldrich Company. Graphene nanosheets (GNS, 98.48% purity) of 50–100 nm thickness were purchased from Angstron Materials, Dayton, Ohio.

Synthesis and Fabrication of the Nanocomposite

5.16 g of 4,4-oxydianiline was dissolved in 100 mL of N-methyl-pyrrolidone (NMP) placed in a three neck round flask. The solution was stirrer continuously for 1 h after which 1.198 g of graphene was added to the solution. This amount of graphene was determined to be equivalent to 10% wt. of the composites. Stirring was maintained at same speed for another 8 h to ensure sufficient dispersion of graphene in the solution. Subsequently, the reaction temperature was reduced to 5 °C after which 5.62 g of pyromellitic dianhydride (PMDA) was added to the mixture with stirring. Stirring was continued for another 10 h. Figure 1 shows a schematic for the synthesis of poly(amic acid). The polymer solution which contains suspended graphene nanosheets was solution cast onto glass substrate and thermally imidized under vacuum at 120 °C for 2 h followed by final curing at 200 °C for 1 h.

Measurements

Dynamic mechanical spectroscopy (DMS) provides a highly sensitive way to study the dynamic mechanical response of a linear viscoelastic material. The response of a polymeric solid under sinusoidal stress is usually expressed in terms of the complex modulus E^* as a function of the frequency and temperature. E^* is composed of its real part (the storage modulus E') and the imaginary part (loss modulus E''). The loss tangent, tan δ or internal friction is the ratio of E'' and E'. Besides the determination of the complex modulus and damping behavior of polymeric materials, DMS is also used to study the following processes (1) curing and cross-linking reactions, (2) the effect of fillers and branching on the glass transition temperature, (3) prediction of lifetime of polymers and composites, (4) determination of temperature for primary and secondary transitions, and (5) determination of the activation energy associated with second order transitions.

In dynamic mechanical measurement a sinusoidal stress σ is applied, and the sinusoidal strain ε is measured over a time period. For a viscoelastic material, strain lags behind the stress because of damping and energy dissipation by the material. The strain ε and stress σ can be expressed as follows:

$$\varepsilon = \varepsilon_\circ \exp(iwt), \tag{1}$$

$$\sigma = \sigma_\circ \exp(i(wt+\delta), \tag{2}$$

where ω is the angular frequency, t is the time, and δ is phase lag.

The complex modulus is expressed as the ratio of sinusoidal stress to sinusoidal strain[17]

$$E^* = \frac{\sigma}{\epsilon} = \frac{\sigma_\circ \exp(i(wt+\delta)}{\varepsilon_\circ \exp(iwt)} = \frac{\sigma_\circ(\cos(wt+\delta)+i(\sin\ wt+\delta))}{\varepsilon_\circ(\cos\ wt + i\sin\ wt)} = \frac{\sigma_\circ}{\varepsilon_\circ}(\cos\delta + i\sin\delta), \tag{3}$$

$$E^* = E' + iE'', \tag{4}$$

where E^* is the complex dynamic mechanical tensile modulus for which the real part $E' = \frac{\sigma_\circ}{\varepsilon_\circ}(\cos\delta)$ is storage modulus and the imaginary part, $E' = \frac{\sigma_\circ}{\varepsilon_\circ}(\sin\delta)$ is the loss modulus which is related to the energy dissipated. $\tan\delta$ is defined as the ratio of energy dissipated to energy stored per cycle of deformation.

$$\tan\delta = \frac{E''}{E'}. \tag{5}$$

The graphene/polyimide composites used in this study contains 10 wt % of graphene nanosheets embedded in the polyimide matrix. Dynamic mechanical spectrometer, DMS used in this study is a DMS EXSTAR 6000, DMS 6100 Module, manufactured by Seiko Instruments, Inc. Dimensions of nanocomposite samples are as follows: 20 mm (L), 6.7 mm (W), and thickness 0.12 mm (t). The polyimide matrix the sample dimensions are 20 mm (L), 6.7 mm (W), and thickness 0.06 mm (t). The strain level for the tension test is 0.01%. DMA mode tension mode applying temperature sweep at various frequencies. The frequency range used is 0.05–100 Hz, and the temperature scan rate is 2.0 °C/min.

Renishaw inVia Raman microscope was used to study the changes in the structure of graphene as a result of reinforcement of polyimide. The scanning electron microscope pictures were taken by using FEI XL30 FEG environmental scanning electron microscope (ESEM model). Samples for ESEM measurements were cut using a razor blade and adhered to a sample holder using carbon tape followed by sputter coating. A denton sputter coater filled with argon gas was used to coat the nonconductive samples with gold palladium for 15 s to achieve conducting samples.

Wide angle X-ray diffraction (WAXD) tests were carried out by using an X'Pert Pro MPD XRD diffractometer with radiation wavelength of 1.54 Å. The 2θ angle range used for each measurement was 5–30°.

RESULTS AND DISCUSSION

Raman Spectroscopy

Figure 2(a–c) show the Raman spectra for (1) polyimide, (2) grapheme, and (3) polyimide–graphene GNS/composites. A characteristic Raman absorption band is observed at 1380 cm^{-1} for polyimide and stems from stretching of C–N bond. The band at 1578 cm^{-1} is due to aromatic –C=C stretching vibration. Another characteristic polyimide peak located at 1780 cm^{-1} is due to the imide cyclic carbonyl, C=O stretching vibration. Graphene shows a strong Raman absorption peak at 1380 cm^{-1}, which is identified to be the carbon D peak due to presence of defects in the carbon crystalline structure. Another Raman characteristic absorption peak for graphene is the G peak associated with the graphitic structure, which is observed at 1580 cm^{-1}. For the polyimide–GNS composite, there is a noticeable shift in the polyimide C–N absorption peak to higher wavenumber to 1388 cm^{-1}. The red shift in the C–N absorption band may be due to structural changes occurring in polyimide in the presence of multilayer graphene sheets. There is also a noticeable overlap and interference between the G peak for graphene and the phenyl –C=C band in polyimide. The cyclic imide carbonyl band was also shifted to higher wavenumber from 1780 to 1785 cm^{-1}, in agreement with the reported shift in the C–N band to higher wavenumber.

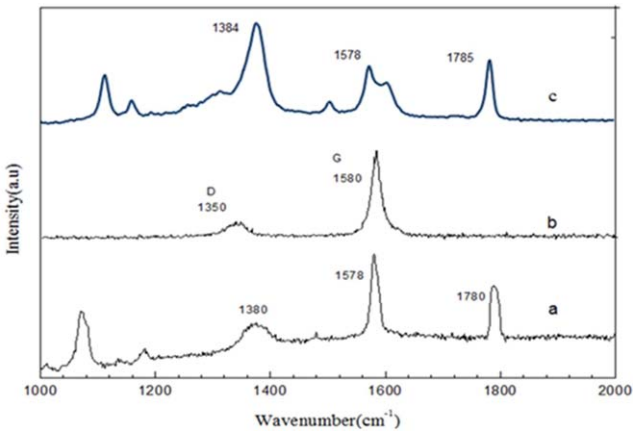

Figure 2. Raman spectra of (a) polyimide, (b) graphene, and (c) polyimide–graphene composite. [Color figure can be viewed in the online issue, which is available at wileyonlinelibrary.com.]

Scanning Electron Microscopy (SEM)

SEM was used to characterize the morphology of the nanocomposites. The micrographs provide valuable information about the dispersion of graphene in polyimide matrix. SEM can also provide a useful insight into the processing-structure–property relationship at the atomistic level. The SEM pictures shows insertion of PI into the galleries with a significant separation between the graphene layers as marked by the arrow. The SEM pictures (Figure 3a,b) suggest that both intercalation and exfoliation of graphene multilayer sheets occurred.

The insertion of graphene in polyimide matrix is responsible for the decrease in the flexibility of polyimide. The morphology of the composite is rough and ridge-like, owing to the 2D geometry of graphene sheets. Figure 3b shows the dispersion of the graphene at higher magnification. The multilayered graphene sheets are intercalated by insertion of poly(amic acid) between graphene sheets during in situ polymerization. The insertion of polyimide into graphene sheets should have a significant impact on the dynamic mechanical behavior of the nanocomposite.

Wide Angle X-ray Diffraction (WAXD) Study

Wide angle X-ray diffraction (WAXD) was used to study the dispersion and structure of the graphene-polyimide composite. X-ray diffraction tests were carried out using a Cu-K radiation source at a wavelength of 1.54 Å and the test was performed in the diffraction angle (2θ) range of 0.5–30°. The d-spacing was calculated by using Bragg's equation, the Bragg equation can be expressed as follows:

$$un\lambda = 2d\sin\theta \ \ (n = 1,\ 2,\ 3,\ \ldots), \tag{6}$$

where λ is the X-ray wavelength, θ is the Bragg angle in degrees, and d is the d-spacing. Figure 4 shows the WAXD diffractographs for polyimide, graphene powder, and polyimide–graphene composite. The WAXD spectrum of graphene powder shows a sharp and strong diffraction peak at a 2θ angle of 26.5°

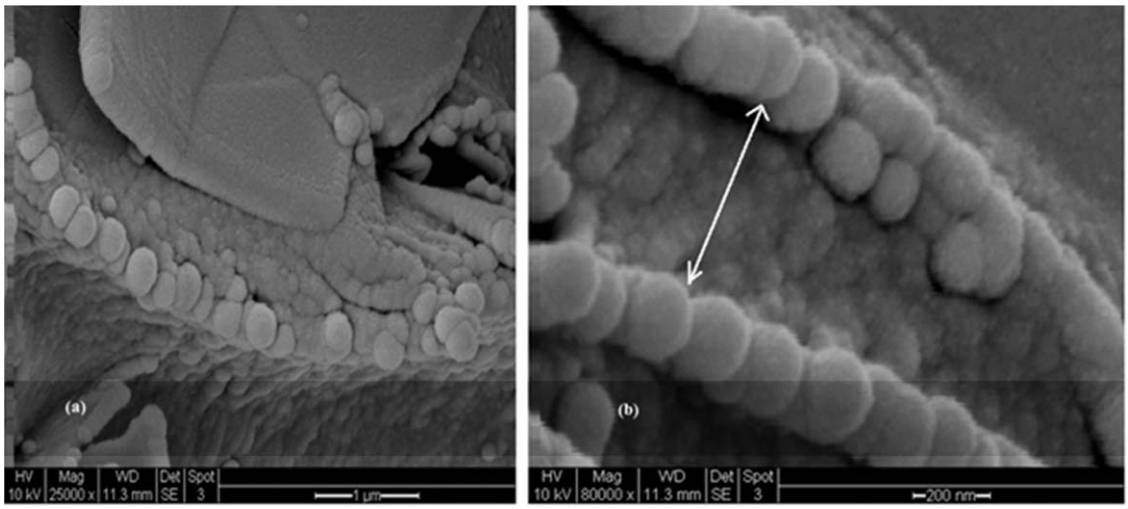

Figure 3. SEM pictures showing cross-sectional morphology of 10% graphene/polyimide at (a) 1 μm and (b) 200 nanometer scale.

which corresponds to the interlayer *d*-spacing 3.36 Å. The WAXD for polyimide does not show any angle diffraction peaks, although there is a broad and weak peak at a diffraction angle, 2θ, of 18° which is believed to be due to the amorphous hallow. The WAXD spectra of the graphene/polyimide composite show a diffraction peaks at a 2θ angle of 26.5° with interlayer spacing, *d* of 3.36 Å which is similar to that observed for graphene powder. It is suggested that the graphene characteristic peak is maintained intact during the formulation of the composite in agreement with the SEM micrographs. A broad and weak diffraction observed at 2θ of 6° is believed to be due to possible interaction of polyimide carbonyl with graphene.

Storage and Loss Moduli

Figure 5 shows the dependence of the storage modulus E' on frequency and temperature, for frequency range of 0.05–100 Hz. The storage modulus, E' increased with increasing applied frequency. For the range of frequency studied, the storage modulus showed significant decrease between 320 and 430 °C due to glass-rubber transition. The decrease of E' as temperature increased in the glass transition region is very gradual at high frequency and sharper at low frequency. The steepest decrease in the storage modulus with increasing temperature occurred between 350 and 430 °C for the composite and 320 and 400 °C for polyimide.

The relaxation behavior of the composite is shown more clearly in Figure 6 where the loss modulus E'' is plotted against temperature as a function of frequency. As the frequency decreased, the α and β transition peaks became sharper and more distinctive. A comparison of variation of loss modulus, E'' with temperature for the composite and polyimide matrix at 1 Hz is shown in Figure 7. The α transition peak for polyimide is stronger and more intense and located at a lower temperature than that for the composite. The trace of variation of the loss modulus with temperature for polyimide shows two major peaks at 100 and 375 °C and a minor but weak peak between 200 and 300 °C. The peak at 100 °C may be due to motion of chain due to presence of solvent and water and may be ascribed to the γ transition. The β transition peak is located between 200 and 300 °C and is due to the fraction of unimidized poly(amic acid). This peak is very weak in the DMS spectrum for neat polyimide at 1 Hz. The intensity of the β transition peak is

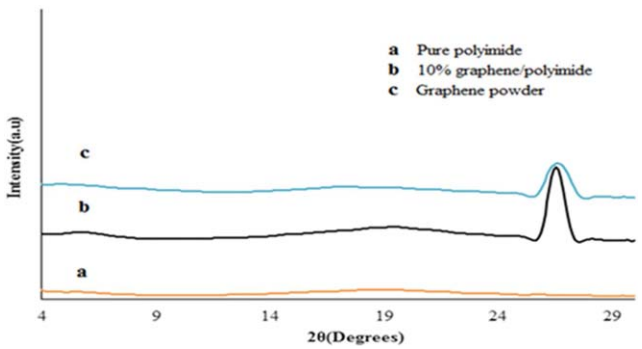

Figure 4. WAXD diffraction spectra for (a) polyimide, (b) graphene/polyimide composite, and (c) graphene. [Color figure can be viewed in the online issue, which is available at wileyonlinelibrary.com.]

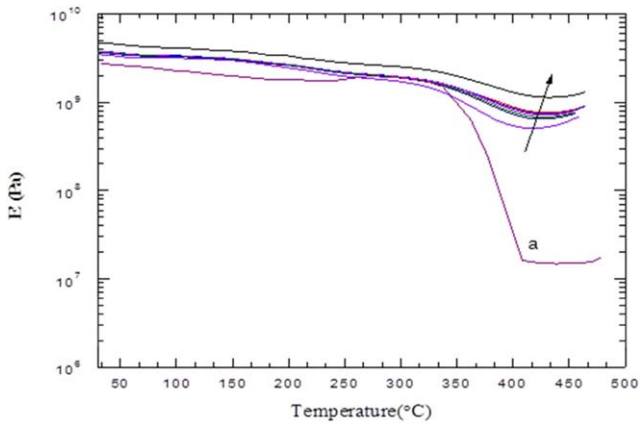

Figure 5. The dependence of the storage modulus, E' for polyimide at 1 Hz [bottom curve, (a)], and polyimide–graphene composite, at a frequency range from 1 to 100 Hz (top curves). [Color figure can be viewed in the online issue, which is available at wileyonlinelibrary.com.]

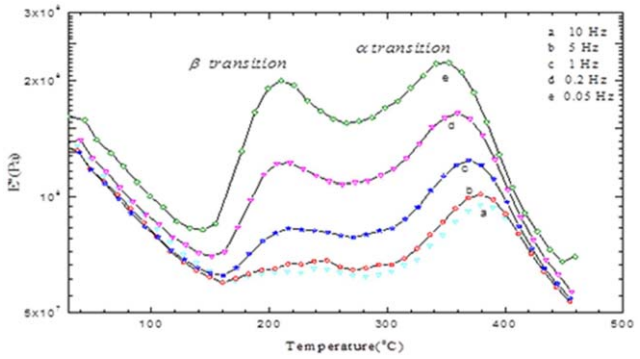

Figure 6. Dependence of loss modulus on temperature and frequency for graphene/polyimide composite. [Color figure can be viewed in the online issue, which is available at wileyonlinelibrary.com.]

strongly dependent on frequency. The ratio of β peak height to α peak height increases with decreasing test frequency due to longer testing time that allows for short range motion of poly(amic acid) block. Indeed at a frequency of 0.05 Hz the ratio of the β to α peak height is nearly one. The glass transition temperature for polyimide was shown to be 375 °C from the log E″ vs. temperature curve (Figure 5). The trace loss modulus against temperature, for the composite shows two intense peaks at 220 and 378 °C at 1 Hz due to the β and α transitions, respectively (Figure 7). There is no noticeable strong peak at 100 °C suggesting minimal segmental motion at this temperature. It is suggested that the β transition for the composites is due to presence of poly(amic acid). The distance separating α and β peaks as well as the ratio of the heights of these two peaks became smaller at shorter test frequencies.

The Cole–Cole type of plot was first developed for studying dielectric behavior of materials,[18] but is also applicable to viscoelastic materials since viscoelasticity has an intrinsic time–energy relationship. Relaxation processes in viscoelastic material can be described by using the Cole–Cole plots. Relaxation occurs whenever polymer chains rearrange themselves to adopt either a lower energy conformation or to fill free volume. The shape of the Cole–Cole plot is affected by factors such as differences in

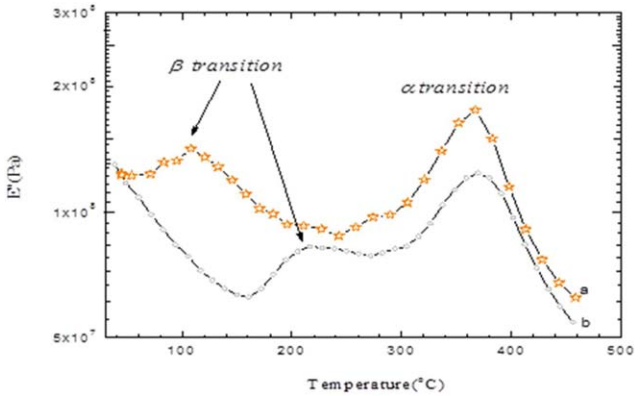

Figure 7. Dependence of loss modulus on temperature at frequency of 1 Hz for (a) polyimide and (b) graphene/polyimide composite. [Color figure can be viewed in the online issue, which is available at wileyonlinelibrary.com.]

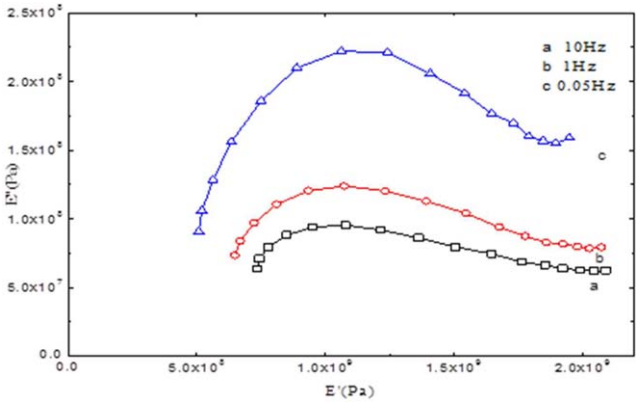

Figure 8. Cole–Cole plot for graphene/polyimide composite at 0.05, 1, and 10 Hz. [Color figure can be viewed in the online issue, which is available at wileyonlinelibrary.com.]

the structure of segmental units within a polymer chain, heterogeneities due to inherent processing characteristic features including (1) molecular weight distribution, (2) free volume distribution, (3) filler concentration, (4) degree of crystallinity and thermomechanical history.[19] Nonsymmetrical semi-circle curve of the Cole–Cole plot for the polymer and polymer composites is indicative of the system's heterogeneity.[20]

The Cole–Cole plot for graphene/polyimide composite is shown in Figure 8 as a function of frequency (0.05–10 Hz). The shape of the Cole–Cole plot for the composites is like a puckered semi-circle that necks and then sharply and trails-off at high modulus end. Graphene nanofillers will constrain the mobility of the polymer chains because of physical and chemical interaction with the matrix. Figure 9 shows comparison of Cole–Cole plot for polyimide and the composite at 1 Hz. The Cole–Cole curves for both system are similar; however, the semicircle made by the Cole–Cole trace for polyimide matrix has a bigger diameter and higher apex, which is consistent with higher loss modulus due to higher dissipated energy for polyimide. The capacitance (approximated to $1/E'$) of the neat polyimide is

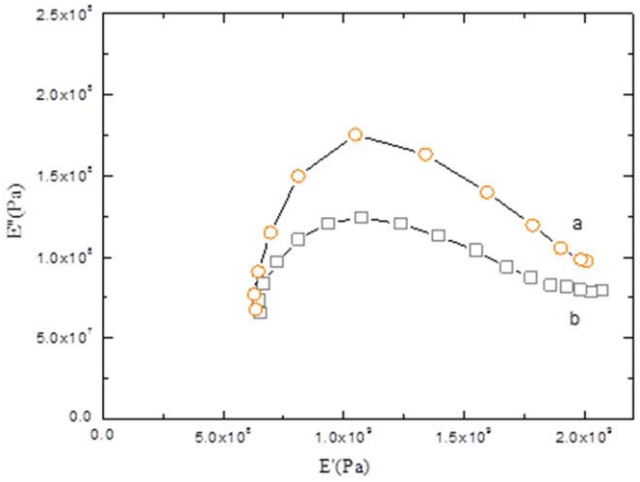

Figure 9. Cole–Cole plot at 1 Hz for (a) polyimide and (b) graphene/polyimide composite. [Color figure can be viewed in the online issue, which is available at wileyonlinelibrary.com.]

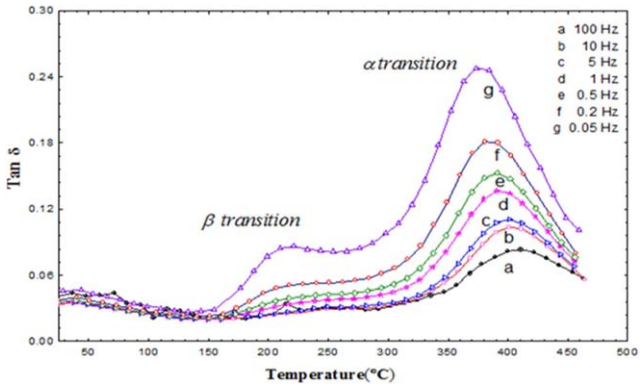

Figure 10. Dependence of tan δ on temperature and frequency for graphene/polyimide composite. [Color figure can be viewed in the online issue, which is available at wileyonlinelibrary.com.]

much higher than that for the composite, which indicates higher damping capacity for polyimide.

Glass Transitions Temperature (α Transition) and β Transition

The α transition of a polymeric material is an important phenomenon and it is related to the thermal energy required for changes in the conformation of the molecules at the microscopic level. The glass transition temperature (T_g) is often referred to as temperature for α transition and it is usually observed as the temperature corresponding to the maximum of tanδ versus temperature curve for the α transition. T_g for graphene/polyimide composite containing 10 wt % of graphene was observed to increase with the increasing frequency as shown in Figure 10. The α transition peak location was shifted to higher temperature as frequency of testing increased, in agreement with the theory of linear viscoelasticity. The T_g for the composites varied between 377 and 419 °C as the test frequencies was varied from 0.05 to 100 Hz. Not only did the tan δ peak for α and β transitions shift to higher temperature, the height of the α and β transitions decreased as the frequency of testing increased as shown in Figure 11. It was also found that the height and location for the β transition peak also varied as the frequency was varied. This trend is similar to that observed for the α transition.

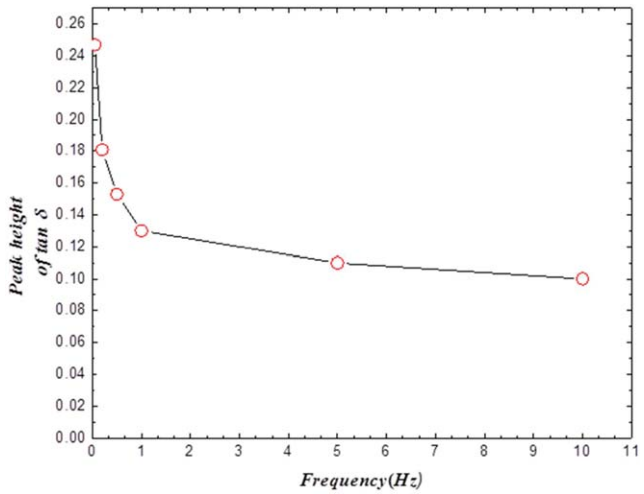

Figure 11. Variation of the tan δ peak height with frequency. [Color figure can be viewed in the online issue, which is available at wileyonlinelibrary.com.]

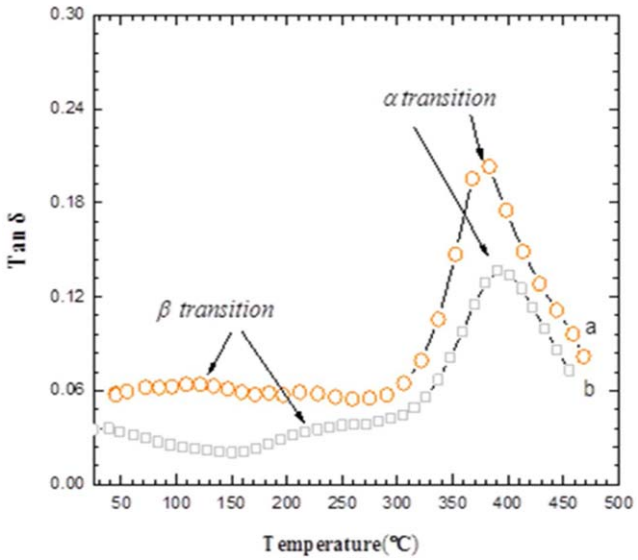

Figure 12. Effect of temperature on tan δ for (a) polyimide and (b) graphene/polyimide composite at 1 Hz. [Color figure can be viewed in the online issue, which is available at wileyonlinelibrary.com.]

The α and β transitions for polyimide are compared to those for the composite at 1 Hz as shown in Figure 12. It is shown that α transition peak for the composite occurred at a higher temperature than that for polyimide; however, the height of α transition peak is much higher for polyimide. Though the presence of graphene lowers the damping ability of polyimide, the nanocomposite showed a remarkably high dissipation peak as indicated by the height of the tan δ peak for α transition of about 0.12 (Figure 12). The low temperature secondary transition peak located at around 100 °C is absent in the tan δ versus temperature curve for the composite (Figure 12) due to enhanced (1) imidization of poly(amic acid) and (2) removal of water and solvent in the presence of graphene.

The activation energy is a measure of the energy barrier that a material must overcome in order to undergo structural reorganization or motion. One of the methods used to calculate the activation energy associated with α and β transition is the Arrhenius method.[21] In the Arrhenius model, the behavior of polymer chains in the glass transition region is explained in frequency terms. The barrier model is based on the idea of two positions (energy minima) separated by a barrier of a given height, i.e., activation energy (E_a). The temperature dependence on frequency can be expressed as given in eq. (7):

$$f = A \exp\left(\frac{-E_a}{RT}\right), \quad (7)$$

where f is the frequency and analogous to the rate constant and A is pre-exponential factor of Arrhenius equation, R is the gas constant, and T is the absolute temperature.[17] The activation energy of both α and β transition can be calculated by using the WLF equation [eq. (9) and eq. (10)].

Table I. DMS Data Based on the Plot of tanδ vs Temperature

f (Hz)	ln f (Hz)	T_α (K)	T_β (K)
0.05	−3.00	650	474
0.2	−1.61	658	483
0.5	−0.69	662	494
1	0.00	668	501
5	1.61	674	506
10	2.30	678	509
100	4.61	692	523

$$\frac{f_1}{f_2} = \frac{A\ \exp\left(\frac{-E_a}{RT_1}\right)}{A\ \exp\left(\frac{-E_a}{RT_2}\right)}, \quad (8)$$

$$\ln\left(\frac{f_1}{f_2}\right) = \frac{E_a}{R}\left(\frac{1}{T_2} - \frac{1}{T_1}\right), \quad (9)$$

$$E_a = -R\frac{d(\ln f)}{d\left(\frac{1}{T_g}\right)}. \quad (10)$$

By analyzing the data from the plot of tan δ against temperature (Table I), one can determine the activation energy by constructing an Arrhenius plot. Arrhenius plot is constructed for both α and β transitions by drawing ln f (Hz) versus $1/T$ (K^{-1}) curve. The plot of ln f against $1/T$ gave a linear relationship whose slope equals $(-E_a/R)$ (Figures 11 and 12). The activation energy E_a was obtained by multiplying the slope of ln f against $1/T$ curve with the gas constant R and 688 and 313 kJ/mol were obtained as the activation energy for α and β transition, respectively. The activation energies obtained in this study are in the range of values reported for an amorphous polymer with aromatic backbone.[22] Comparison of the activation energy for relaxation for polyimide and the composite shows that the energy barrier for chain relaxation is higher for the composite than polyimide, when tested under similar conditions (Figures 13 and 14). The fit for the β transition is not as good as that for the α transition due to the difficulty of locating the exact position of the β transition peak from the broad and weak tan δ versus temperature peaks for β transition.

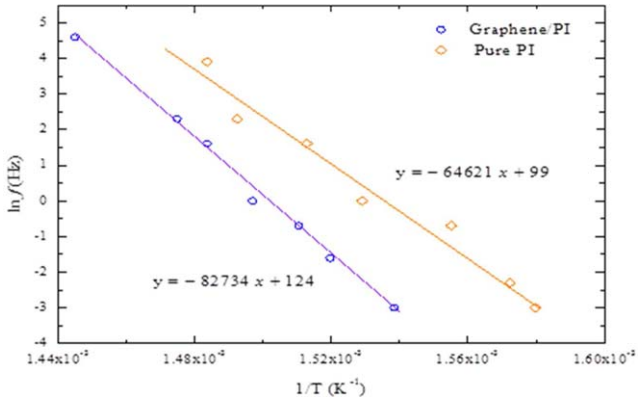

Figure 13. Arrhenius plot for α transition for polyimide (top) and graphene/polyimide composites (bottom). [Color figure can be viewed in the online issue, which is available at wileyonlinelibrary.com.]

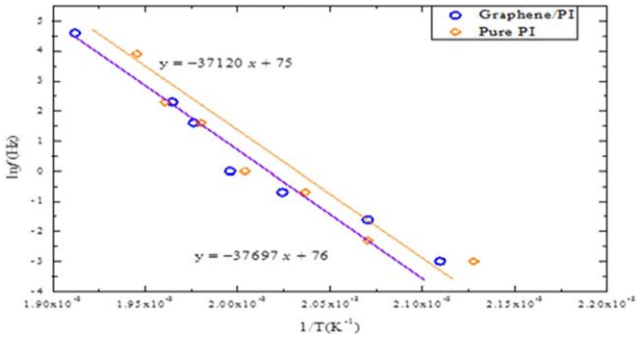

Figure 14. Arrhenius plot for β transition for polyimide (top) graphene/polyimide composite (bottom). [Color figure can be viewed in the online issue, which is available at wileyonlinelibrary.com.]

CONCLUSIONS

Raman spectrum for graphene/polyimide composite shows a noticeable shift in the polyimide C–N absorption peak to higher wavenumber to 1388 cm^{-1} due to structural changes occurring in polyimide in the presence of graphene. Raman spectroscopy also shows an overlap between the graphitic G peak in graphene and the phenyl (aromatic) band in polyimide due to lattice matching of the aromatic units present in both graphene and polyimide. The tan δ dependence of on frequency and temperature is much more pronounced at lower test frequency where the tan δ peak height for both the α and β transition are more intense and sharp.

The activation energy for the glass transition was determined to be 688 and 537 kJ/mol for graphene/polyimide composite and neat polyimide, respectively, which are significantly higher than those for the β transition of 313 and 309 kJ/mol for the composite and matrix, respectively. The nonsymmetrical nature of the Cole–Cole plot affirms the heterogeneity of both the nanocomposite and polyimide.

ACKNOWLEDGMENTS

We are grateful for the financial support and opportunity for this research, funded by the National Science Foundation (NSF) (grant number CMMI-0758656).

REFERENCES

1. Ha, C.-S.; Mathews, A. S. In Advanced Functional Materials; Springer: Berlin, **2011**; pp 1–36.
2. Ghosh, M. In Polyimides: Fundamentals and Applications; CRC Press: New York, **1996**; Vol. *36*.
3. Sroog, C. E. *J. Polym. Sci. Macromol. Rev.* **1976**, *11*, 161.
4. Ahmad, Z.; Mark, J. E. *Chem. Mater.* **2001**, *13*, 3320.
5. Ward, I. M.; Sweeney, J. In Mechanical Properties of Solid Polymers; Wiley: New York, **2012**.
6. R. M. Jones, In Mechanics of Composite Materials, 2nd ed.; Taylor and Francis: Philadelphia, **1982**.

7. Ghosh, M. K.; Mittal, K. L., Eds.; In Polyimides: Fundamentals and Applications; Marcel Dekker: New York, **1996**.
8. Fang, X. Z.; Yang, Z. H.; Zhang, S. B.; Gao, L. X.; Ding, M. X. *Polymer* **2004**, *45*, 2539.
9. Longun, J.; Iroh, J. O. *Carbon* **2012**, *50*, 1823.
10. Yoonessi, M.; Ying, S.; Daniel, A. S.; Marisabel, L.-C.; Dean, M. T.; Weiss, R. A.; and Michael, A. M. *ACS Nano* **2012**, *6*, 7644.
11. Zhang, L.-B.; Jin-Qing, W.; Hong-Gang, W.; Ye, X.; Zhao-Feng, W.; Zhang-Peng , L.; Yong-Juan, M.; and Sheng-Rong, Y. *Compos. Part A* **2012**, *43*, 1537.
12. Ferry, J. D. In Viscoelastic Properties of Polymers, 1st ed.; Wiley: New York, **1961**; Chapter 11.
13. Maxwell, A. S.; Monnerie, L.; Ward, I. M. *Polymer* **1998**, *39*, 6851.
14. Yano, O.; Wada, Y. *J. Polym. Sci., Part A* **1971**, *9*, 669.
15. Tyan, H.-L.; Liu, Y.-C.; Wei, K.-H. *Polymer* **1999**, *40*, 4877.
16. Rana, D.; Sauvant, V.; Halary, J. L. *J. Mater. Sci.* **2002**, *37*, 5267.
17. Ward, I. M.; Dennis, W. H. In An Introduction to the Mechanical Properties of Solid Polymers; John Wiley and Sons: New York, **1993**; Chapter 6, pp 84–108.
18. Cole, K. S.; Cole, R. H. *J. Chem. Phys.* **1941**, *9*, 341.
19. Oréfice, R. L.; Hench, L. L.; Brennan, A. B. *J. Braz. Soc. Mech. Sci.* **2001**, *23*, 1.
20. Romanzini, D.; Alessandra, L.; Heitor, L. O.; Sandro, C. A.; and Ademir, J. Z. *Mater. Des.* **2013**, *47*, 9.
21. Bicerano, J. In Prediction of Polymer Properties, 2nd ed.; Marcel Dekker Inc.: New York, **1996**.
22. Bessonov, M. I.; Kuznetsov, N. P.; Adrova, N. A.; and Florinskii, F. S. *Polym. Sci. USSR* **1974**, *16*, 2425.